Cooling Curve Analysis as an Alternative to Dilatometry in Continuous Cooling Transformations

JOHN W. GIBBS, CHRISTIAN SCHLACHER, ATA KAMYABI-GOL, PETER MAYR, and PATRICIO F. MENDEZ

Dilatometry and cooling curve analysis (CCA) are two methods of determining the evolution of a phase transformation with temperature. The two methods are similar conceptual in that they take an indirect measure of the transformation and extract phase fraction information from it; however, the differences between the two methods typically makes one method better suited to analyzing a given transformation. However, without a quantitative comparison between the two methods, it is difficult to use them interchangeably. We address this by presenting a quantitative comparison of CCA and dilatometry for a martensitic transformation in a 9Cr3W3CoVNb steel. The resulting phase fraction data matches very well, within 5 K (5 °C) for any given phase fraction. This paper also extends to the quantitative methodology of calorimetry to the analysis of dilatometric data, with results comparable to ASTM A1033-10, but with expected higher accuracy by accounting by variable thermal expansion coefficients.

DOI: 10.1007/s11661-014-2603-8

I. INTRODUCTION

DILATOMETRY is commonly used to quantify the progress of solid-state phase transformations during continuous heating or cooling because it gives accurate and simple to interpret results that indicate start and finish temperatures of the transformation, relative phase fraction as a function of temperature and, when combined with information about the relative densities of the two phases, it can be used to determine the absolute amount of second phase formed as a function of temperature.[1–4]

One of the downsides of dilatometry is that it requires specialized equipment to make precise length/diameter measurements; this can be a limitation if one does not have access to a dilatometer or if a dilatometer is incompatible with a concurrent experiment (*e.g.*, a tensile test or a synchrotron experiment). One proposed alternative method that has a significantly simpler experimental setup is cooling curve analysis (CCA); a technique that involves measuring the temperature of a sample as it cools and transforms, then using the transformation-induced deviations from single-phase cooling behavior to determine the phase fraction evolution.[5,6]

The goal of both dilatometry and CCA is to obtain phase fraction evolution information of a material as it undergoes monotonic heating or cooling. Because of the similarities in the results and sample conditions during the experiment, dilatometry and CCA can be seen as complimentary techniques; however, there has never been a published, quantitative comparison of the two. This work is intended to provide an initial comparison for one type of transformation.

For the comparison between the two methods, an austenite to martensite transformation is used because this is a common transformation to be analyzed using dilatometry. Dilatometry and CCA techniques are well suited to this type of transformation because both methods provide information on both the formation temperature and the amount formed as a function of temperature. The properties of the transformed martensite depend on the temperature at which it forms and the properties of the alloy depend upon the properties and amount of martensite present.

While this one comparison does not make for a comprehensive comparison between the two methods, the combination of the derivations of the two methods and the results should make it possible to determine which of the two methods presents a better set of compromises for almost any given transformation.

Although the following methods are not the focus of this paper, it is important to consider alternate techniques that are available to measure phase fraction and also to note how these techniques compare to dilatometry and CCA. Differential thermal analysis (DTA) methods,[7] including single-sensor DTA,[8] are useful for measuring the start and finish temperatures of a transformation but not the phase fractions. Differential scanning calorimetry (DSC) can be used for very precise measures of the enthalpy evolution of a transformation, which can be used to calculate phase fraction evolution similarly to CCA methods. A major drawback associated with DTA and DSC is that the small sample size is not statistically representative of real size components

JOHN W. GIBBS, Ph.D. Student, is with Northwestern University, Evanston, IL. Contact e-mail: john@gibbsium.org CHRISTIAN SCHLACHER, Ph.D. Student, is with the Graz University of Technology, Graz, Austria. ATA KAMYABI-GOL, Ph.D. Student, and PATRICIO F. MENDEZ, Professor, are with the University of Alberta, Edmonton, Canada. PETER MAYR, Professor, is with the Technische Universität Chemnitz, Chemnitz, Germany.

Manuscript submitted April 14, 2014.

Published online: 15 October 2014

and the rates of heating and cooling are more restricted than in CCA.[9]

There are also indirect ways of measuring phase fraction evolution, such as measuring the electrical conductivity[10] or magnetic properties[11] and correlating their change to a change in phase fraction, similarly to how length change is used as a proxy for phase change information in dilatometry.[12] It is important to note that the CCA method that is presented here is just one of several CCA techniques that are all based on similar principles.[9,13]

The innovative aspect presented in this paper resides on the rigorous mathematical formulation which allows for the extension of this methodology to other problems, including multiple simultaneous transformations. This paper has also extended the mathematical framework to provide a rigorous analysis of dilatometric data.

II. DILATOMETRY

The dilatometry analysis presented here involves developing a model that contains the collected data and terms that are either dependent on temperature or phase fraction (but not both); then using the collected data to determine values for the temperature dependent terms; and finally, solving for the phase fraction.

This new methodology for analyzing dilatometry data is proposed that is consistent with typical line-drawing techniques but is more mathematically rigorous. It also provides a unified framework that can also be used for the CCA that is presented in the next section.

A. *Material Model*

Considering a two phase system, the total volume of the sample is $V = V_\alpha + V_\beta$. With the assumption of a constant cross section A for a given sample, $V = LA$, where L is the length of the sample. Using the definition of density, it can be stated:

$$LA = \frac{m_\alpha}{\rho_\alpha} + \frac{m_\beta}{\rho_\beta} \quad [1]$$

The nomenclature used throughout this paper is described in Table I. To obtain an expression for phase fraction evolution, the mass of the phases are separated into total mass of the system and phase fraction by weight in Eq. [1]:

$$L = m(f_\alpha \lambda_\alpha + f_\beta \lambda_\beta) \quad [2]$$

where m is the total mass of the sample, f_α and f_β are, respectively, the mass fractions of the α and β phases, $\lambda_\alpha = (\rho_\alpha A)^{-1}$ and $\lambda_\beta = (\rho_\beta A)^{-1}$. Equation [2] is differentiated with respect to temperature to obtain:

$$\frac{dL}{dT} = m\left(f_\alpha \frac{\partial \lambda_\alpha}{\partial T} + \frac{\partial f_\alpha}{\partial T}\lambda_\alpha\right) + m\left(f_\beta \frac{\partial \lambda_\beta}{\partial T} + \frac{\partial f_\beta}{\partial T}\lambda_\beta\right). \quad [3]$$

Rearranging terms and keeping in mind that in a two phase system $f_\alpha = 1 - f_\beta$ and $df_\beta = -df_\alpha$ gives:

Table I. List of Terms and Symbols Used in the Dilatometry and Cooling Curve Analysis

Symbol	Name	Units
Common terms		
α	name of the high temperature phase	
β	name of the low temperature phase	
ρ_i	specific density of phase i	g/μm^3
t	time	s
T	measured temperature of the sample	K
m	total mass of the sample	g
m_i	total mass of phase i	g
f_i	mass fraction of phase i	g/g
n	index number	
Dilatometry specific terms		
A	cross-sectional area of the sample	μm^2
$\bar{h}$	average heat-transfer coefficient over the sample	W/m^2 K
K	heat transfer coefficient of the sample	W/m^2 K
L	measured length of the sample	μm
L_i	total length of phase i	μm
λ_i	specific length of phase i	μm/g
$\mathcal{L}_\alpha$	term defined in Eq. [5]	μm/K
$\mathcal{L}_\beta$	term defined in Eq. [6]	μm/K
$C_{\Delta\lambda}$	term defined in Eq. [7]	μm
CCA specific terms		
H	extrinsic enthalpy of the system	J
H^*	intrinsic specific enthalpy of the sample or phase	J/g
ΔH	latent heat of transformation	J/g
c_p^i	specific heat capacity of phase i	J/g K
λ_i	specific length of phase i	μ m/g
γ_α	term defined in Eq. [17]	s
γ_β	term defined in Eq. [18]	s
$C_{\Delta H}$	term defined in Eq. [19]	K s

$$\frac{dL}{dT} = m\frac{\partial \lambda_\alpha}{\partial T}(1 - f_\beta) + m\frac{\partial \lambda_\beta}{\partial T} f_\beta - m(\lambda_\alpha - \lambda_\beta)\frac{\partial f_\beta}{\partial T} \quad [4]$$

This equation contains terms that are collected data (L, T), constant (m), dependent on temperature (λ_α, λ_β) or dependent on phase fraction (f_β).

B. *Determining Phase Fraction Independent Terms*

In each of the three terms on the right hand side of Eq. [4], there are groups of variables that are only functions of temperature; these are grouped together and replaced with new variables to simplify the nomenclature:

$$\mathcal{L}_\alpha = m\frac{\partial \lambda_\alpha}{\partial T} \quad [5]$$

$$\mathcal{L}_\beta = m\frac{\partial \lambda_\beta}{\partial T} \quad [6]$$

$$C_{\Delta\lambda} = m(\lambda_\alpha - \lambda_\beta) \quad [7]$$

Substituting these quantities into Eq. [4] results in:

$$\frac{dL}{dT} = \mathcal{L}_\alpha(1 - f_\beta) + \mathcal{L}_\beta f_\beta - C_{\Delta\lambda}\frac{\partial f_\beta}{\partial T}, \quad [8]$$

where the $\mathcal{L}$ terms are functions of temperature. The variations of $C_{\Delta\lambda}$ with temperature are proportional to the difference $\mathcal{L}_\alpha - \mathcal{L}_\beta$. For typical materials, $\mathcal{L}_\alpha - \mathcal{L}_\beta$ is much smaller than either $\mathcal{L}_\alpha$ or $\mathcal{L}_\beta$, and $C_{\Delta\lambda}$ will be considered as independent of temperature. Significantly, by defining these grouped quantities that can be determined from the experimental data, there are no material parameters that have to be known *a priori*; the length-temperature data are the only inputs that are required to perform this analysis.

In determining the values of these terms, it is important to keep in mind what the phase fractions represent. For some transformations, such as solidification, the definition is very straight forward: f_α is the liquid fraction and f_β is the solid fraction and the system will start at $f_\beta = 0$ and finish at $f_\beta = 1$. For other transformations, such as martensite formation from austenite, it is mathematically more convenient to let f_α represent the fraction of pre-transformation constituent and f_β represent the fraction of post-transformation product. For example, in a martensite transformation that yields a maximum of 40 pct martensite that is half way through the transformation, there would be 20 pct martensite and $f_\beta = 0.5$.

Using this definition of the phase fractions, the values for the $\mathcal{L}$ terms can be determined by considering Eq. [8] either before or after the transformation takes place. Before the transformation, when the system is comprised entirely of α and no transformation is occurring ($f_\beta = 0$ and $\partial f_\beta / \partial T = 0$), Eq. [8] becomes:

$$\frac{\mathrm{d}L}{\mathrm{d}T} = \mathcal{L}_\alpha \qquad [9]$$

A similar argument can be used to relate the measured length (L) to $\mathcal{L}_\beta$ after the transformation has occurred and these terms can be easily computed from the measured data.

Determining a value for $C_{\Delta\lambda}$ is done by first assuming a reasonable value, then proceeding with this analysis to obtain a phase fraction evolution curve that begins at $f_\beta = 0$ and ends at some value of f_β other than 1. Since the transformation proceeds to $f_\beta = 1$ by definition, the calculated values of f_β after the transformation can be used to make an improved evaluation of $C_{\Delta\lambda}$. This process is iterated until $f_\beta = 1$ after the transformation is complete.

C. *Determining Phase Fractions*

Equation [8] can be rearranged to pose it as a differential equation for phase fraction evolution as follows:

$$\frac{\partial f_\beta}{\partial T} = \frac{1}{C_{\Delta\lambda}}\left[\mathcal{L}_\alpha\left(1 - f_\beta\right) + \mathcal{L}_\beta f_\beta - \frac{\mathrm{d}L}{\mathrm{d}T}\right]. \qquad [10]$$

Equation [10] can be numerically integrated, starting from an initial condition of $f_\beta = 0$, using an explicit Euler integration scheme as shown below:

$$f_\beta^{n+1} = f_\beta^n + \frac{T^{n+1} - T^n}{C_{\Delta\lambda}}\left[\mathcal{L}_\alpha^n\left(1 - f_\beta^n\right) + \mathcal{L}_\beta^n f_\beta^n - \frac{L^{n+1} - L^n}{T^{n+1} - T^n}\right]. \qquad [11]$$

III. COOLING CURVE ANALYSIS

The thermal analysis technique presented here was originally presented in References 5, 6. This technique is similar to that presented for dilatometry in which a model is proposed that describes the enthalpy of the sample using terms that are functions of either temperature or phase fraction, solving for the temperature dependent terms, then determining the phase fraction. The primary difference between the dilatometry and CCA is that the dilatometry model is based on the length of the sample, which is measured directly, whereas the thermal model is based on the enthalpy of the sample, which must be inferred by using a heat transfer model.

A. *Thermal Model*

The thermal model assumes two phases are present and the total enthalpy of the sample can be described by a sum of the enthalpies of the individual phases ($H = H_\alpha + H_\beta$). Similarly to the dilatometry analysis, the enthalpy terms are split to separately account for changes in the enthalpy of the phase that are due to a change in the amount of the phase and changes that are due to variations in the specific enthalpy of the phase.

$$H = m_\alpha H_\alpha^* + m_\beta H_\beta^* \qquad [12]$$

where H is the extrinsic enthalpy of the sample and the H_i^* terms are enthalpies per unit mass of the phases. By further splitting the masses of the individual phases into total system mass and phase fraction, and differentiating Eq. [12] with respect to temperature, the following equation is obtained:

$$\frac{\mathrm{d}H}{\mathrm{d}T} = m\left(\frac{\partial f_\alpha}{\partial T}H_\alpha^* + f_\alpha\frac{\partial H_\alpha^*}{\partial T}\right) + m\left(\frac{\partial f_\beta}{\partial T}H_\beta^* + f_\beta\frac{\partial H_\beta^*}{\partial T}\right). \qquad [13]$$

This equation can be simplified by rearranging terms and using the properties of a two phase system similar to what was done in the dilatometry section. It is also convenient to replace the enthalpy differentials with thermodynamic quantities, namely specific heat capacity (c_p) and heat of transformation (ΔH^*).

$$\frac{\mathrm{d}H}{\mathrm{d}T} = mc_\mathrm{p}^\alpha\left(1 - f_\beta\right) + mc_\mathrm{p}^\beta f_\beta - m\Delta H^*\frac{\partial f_\beta}{\partial T} \qquad [14]$$

To relate $\mathrm{d}H/\mathrm{d}T$ to the observed temperatures in the experiment, a heat transfer relationship is used. Depending on the dominant cooling mechanism, a relationship describing conduction, convection, or radiation is used. While this requirement for consistent cooling conditions does not allow for as much freedom of cooling rates as dilatometry, it is quite adaptable since the cooling rate of the sample can vary by orders of magnitude depending on sample size and geometry and ambient air conditions. For this particular set of experiments, the following convection dominant equation is used:

$$\frac{\mathrm{d}H}{\mathrm{d}t} = \bar{h}A(T - T_\infty). \quad [15]$$

This is related to Eq. [14] by multiplying the left hand side of Eq. [15] by $(\mathrm{d}T/\mathrm{d}t)^{-1}$ to obtain a $\mathrm{d}H/\mathrm{d}T$ term, then replacing $\mathrm{d}H/\mathrm{d}T$ by the right hand side of Eq. [14] to get:

$$\frac{dT}{dt}\left[mc_\mathrm{p}^\alpha(1 - f_\beta) + mc_\mathrm{p}^\beta f_\beta - m\Delta H^* \frac{\partial f_\beta}{\partial T}\right] = \bar{h}A(T - T_\infty) \quad [16]$$

B. *Determining Phase Fraction Independent Terms*

In its present form, Eq. [16] contains six unknowns: m, ΔH^*, c_p^α, c_p^β, $\bar{h}$, and A. It is intractable to solve for each of them individually. Since all these variables are functions of temperature and not phase fraction, it is possible to combine them into just three variables using the following definitions:

$$\gamma_\alpha = \frac{mc_\mathrm{p}^\alpha}{\bar{h}A} \quad [17]$$

$$\gamma_\beta = \frac{mc_\mathrm{p}^\beta}{\bar{h}A} \quad [18]$$

$$C_{\Delta H} = \frac{m\Delta H^*}{\bar{h}A} \quad [19]$$

Using these variables, Eq. [16] becomes:

$$\gamma_\alpha \frac{\mathrm{d}T}{\mathrm{d}t}(1 - f_\beta) + \gamma_\beta \frac{\mathrm{d}T}{\mathrm{d}t} f_\beta - C_{\Delta H} \frac{\mathrm{d}f_\beta}{\mathrm{d}t} = (T - T_\infty), \quad [20]$$

where γ_α and γ_β are functions of temperature due to the temperature dependence of the specific heat capacity and $C_{\Delta H}$ is a constant. These new parameters can be evaluated by considering Eq. [20] when no transformation is occurring. Similarly to the dilatometry analysis, this step is significant because it allows the three new terms to be determined from the experimental data so none of the terms in Eqs. [17], [18] or [19] need to be known *a priori*.

Equation [20] can be used to determine the values of these new terms. For example, before the transformation begins $f_\beta = 0$ and $\mathrm{d}f_\beta/\mathrm{d}t = 0$ and Eq. [20] becomes:

$$\gamma_\alpha = \left(\frac{\mathrm{d}T}{\mathrm{d}t}\right)^{-1}(T - T_\infty). \quad [21]$$

This equation provides a unique relationship between the collected temperature data and the fitted γ_α variable. A similar procedure can be done after the transformation occurs to obtain a relationship for fitting γ_β. To determine a value for $C_{\Delta H}$, a similar procedure is used to the dilatometry analysis is used.

C. *Determining Phase Fractions*

To determine phase fractions, Eq. [20] is rearranged to isolate $\mathrm{d}f_\beta/\mathrm{d}t$ as follows:

$$\frac{\mathrm{d}f_\beta}{\mathrm{d}t} = \frac{1}{C_{\Delta H}}\left[\gamma_\alpha \frac{\mathrm{d}T}{\mathrm{d}t}(1 - f_\beta) + \gamma_\beta \frac{\mathrm{d}T}{\mathrm{d}t} f_\beta - (T - T_\infty)\right]. \quad [22]$$

This equation is then discretized and numerically integrated using an explicit Euler integration scheme with an initial condition of $f_\beta = 0$:

$$f_\beta^{n+1} = f_\beta^n + \frac{t^{n+1} - t^n}{C_{\Delta H}}\left[\gamma_\alpha \frac{T^{n+1} - T^n}{t^{n+1} - t^n}\left(1 - f_\beta^n\right) + \gamma_\beta \frac{T^{n+1} - T^n}{t^{n+1} - t^n} f_\beta^n - \left(T^{n+1} - T_\infty\right)\right]. \quad [23]$$

IV. EXPERIMENTAL SETUP

A simultaneous dilatometry and CCA experiment was performed on a 9Cr3W3CoVNb steel with controlled additions of 120 ppm boron and 130 ppm nitrogen produced by vacuum induction melting (VIM) in order to compare the results between the two methods. Table II shows the exact chemical composition of the steel in weight percent.

After the melting process the ingot (110 by 110 mm^2) was rolled to 20-mm-thick plates. The heat treatment consisted of normalizing at 1423 K (1150 °C) for 1 hour followed by tempering at 1043 (770 °C) for 4 hours. To reveal the microstructure of the base material (before dilatometry) the surface of the samples was subsequently ground using silicon carbide paper down to grit 4000 and polished in two steps using a cloth coated with 3 and 1 μm diamond suspensions. The polished samples were etched using a modified LBII etchant that is made up of 100 mL distilled water, 0.75 g ammonium hydrogenfluoride, 0.90 g potassium disulfide.[14] This is a color etchant that reveals martensitic lath structure, prior austenite grain boundaries and precipitates. Optical micrographs of the base materials are shown in Figure 1. The base material in Figure 1(a) shows a tempered martensitic structure with a homogeneous polygon prior austenite grain structure with an average grain size of 300 μm.

A. *Dilatometry Setup*

For the dilatometry investigations a Bahr DIL-805/D dilatometer was utilized. Cylindrical specimens of the 9Cr3W3CoVNb base material with a diameter of 4 mm

Table II. Chemical Composition of 9Cr3W3CoVNbBN Test Melt in Weight Percent (Balance Fe)

Element	C	Si	Mn	Cr	W	V	Nb	Co	Al	B	N
Amount	0.090	0.30	0.51	9.26	2.92	0.20	0.050	2.88	0.004	0.0114	0.0100

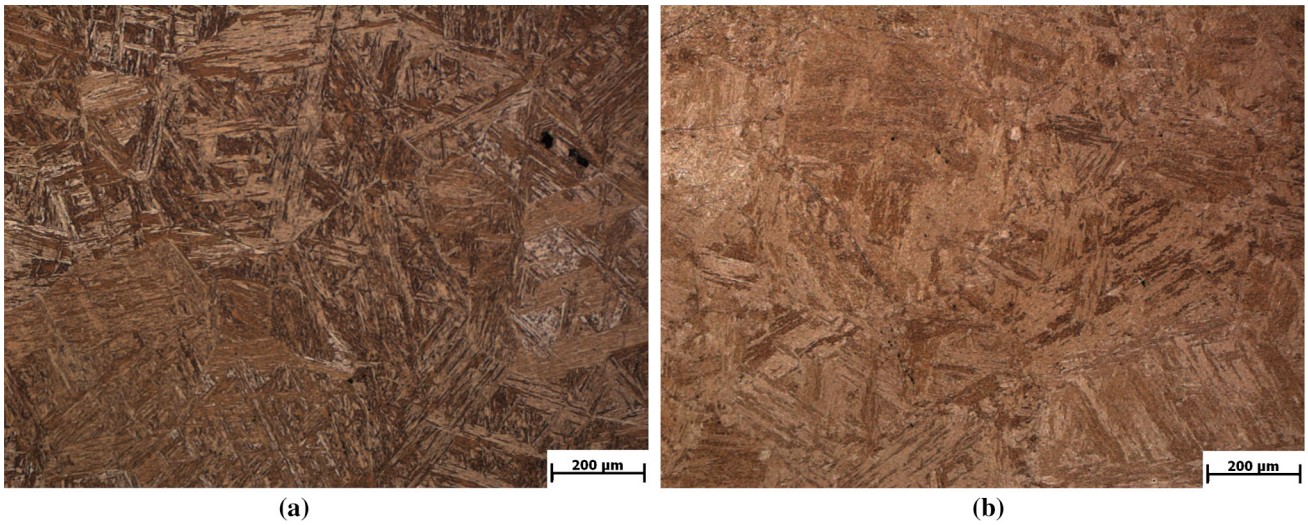

Fig. 1—Optical micrographs of the 9Cr3W3CoVNb steel microstructure before (*a*) and after (*b*) dilatometry.

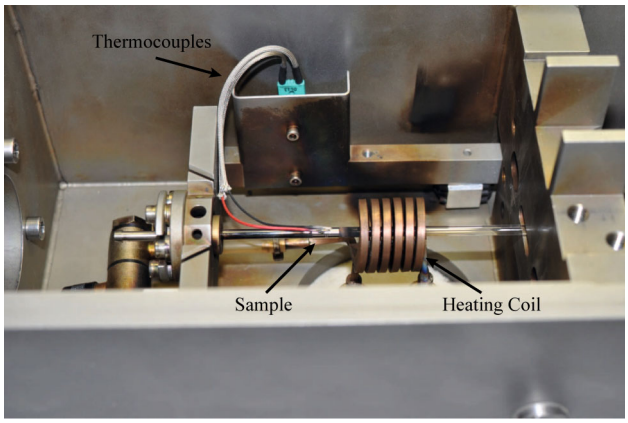

Fig. 2—Experimental setup of the dilatometer sample chamber.

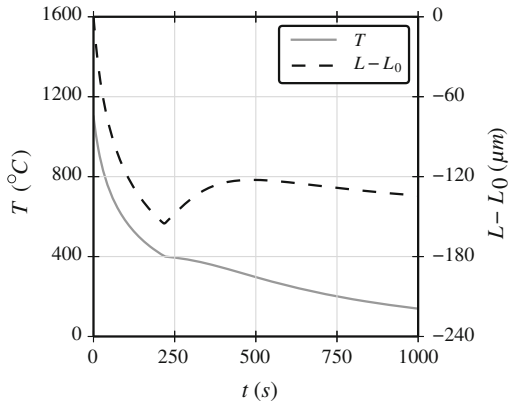

Fig. 3—Temperature and length change relative to the room temperature length.

and a length of 10 mm were used. Figure 2 shows the experimental setup of the dilatometer and the sample chamber.

The dilatometry temperature cycle is characterized by a heating rate of 10 K/s, a peak temperature of 1373 K (1100 °C), a holding time of 3 seconds, and free cooling. The dilatometer is used to precisely record the change in length of the sample as it is heated and cooled with time. In addition, variations of temperature with time are recorded simultaneously. The resulting length change and temperature measurements are shown in Figure 3.

After the dilatometry experiments, the microstructure of the samples were analyzed again. Figure 1(b) represents the final microstructure of the steel samples after the thermal cycle. The material shows a martensitic microstructure with approximately 4 pct retained austenite (based on X-ray diffraction data discussed in detail in References 15 through 17). The prior austenite grain boundaries are more difficult to observe compared to the base material shown in Figure 1(a) primarily due to the formation of virgin martensite.[17]

V. ANALYSIS AND RESULTS

To determine values for the temperature dependent terms ($\mathcal{L}$ in Eqs. [5] and [6] and γ in Eqs. [17] and [18]), temperature ranges that relate to before and after the transformation occurs must be defined so that the terms relating to the α phase (austenite in this case) are fit where only α is present and the same for terms relating to the β phase (martensite in this case). The temperature range considered for the region where only austenite is present was 698 K to 1123 K (425 °C to 850 °C). For the region where martensite is the dominant phase present during cooling, the temperature range considered was (373 K to 473 K) 100 °C to 200 °C.

Results from the single phase regions in the cooling curve can be seen in Figure 4. The higher temperature curve in the CCA plot representing γ_α is fitted to the data between 1123 K and 698 K (850 °C and 425 °C) and was best captured by using a second-order polynomial while the lower temperature curve is fitted between 473 K and 373 K (200 °C and 100 °C) and was captured by using a straight line as suggested by References 5, 6.

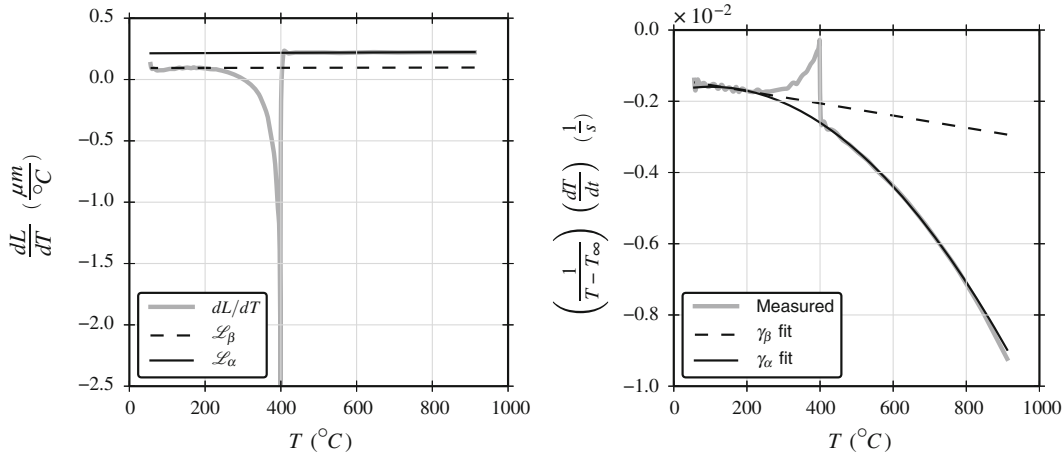

(a) Dilatometry **(b)** CCA

Fig. 4—Fitting of $\mathcal{L}$ and γ terms for dilatometry and CCA, respectively.

Table III. Values for the Parameters Used in Curve Fittings

Parameter	Value	Units
γ_α	$-1.1 \times 10^{-8} T^2 + 2.3 \times 10^{-6} T - 1.7 \times 10^{-3}$	1/s
γ_β	$-1.7 \times 10^{-6} T - 1.4 \times 10^{-3}$	1/s
$C_{\Delta H}$	$+4.7 \times 10^{+4}$	K s
$\mathcal{L}_\alpha$	$+1.2 \times 10^{-5} T + 2.1 \times 10^{-1}$	μm/K
$\mathcal{L}_\beta$	$-4.4 \times 10^{-6} T + 9.4 \times 10^{-2}$	μm/K
$C_{\Delta\lambda}$	$+5.1 \times 10^{+1}$	μm

The high temperature CCA fit was likely affected by radiation heat loss, which is proportional to T^4, instead of T as in the case of convection. This causes deviations from linearity in γ_α which was best captured with a second-order polynomial rather than a straight line. In the case of the dilatometry plot, both $\mathcal{L}_\alpha$ and $\mathcal{L}_\beta$ were best captured using linear functions of temperature. The values for the parameters used in the curve fittings are presented in Table III.

The evolution of the martensite fraction with time can be calculated using three separate methods: (a) classic "lever" method as per ASTM A1033-10; (b) using the approach mentioned in Section II–C (dilation data); (c) using the approach proposed in Section III–C (temperature data). Figure 5(a) compares the evolution of the martensite fraction with temperature obtained from both calorimetry and dilatometry methods. It can be seen in Figure 5 that martensite formation starts around 673 K (400 °C) and ends close to 523 K (250 °C). This figure also includes the martensite fraction obtained from the experimental graph using ASTM A1033-10 standard method for graphical estimates of transformation progress.[18] Figure 5(b) clearly shows that both calorimetry and dilatometry are powerful tools in predicting the evolution of martensite fraction with time. The temperature difference (ΔT_{max}) between the dilatometry and calorimetry curves observed in Figure 5(b) is explained in detail in the Appendix section.

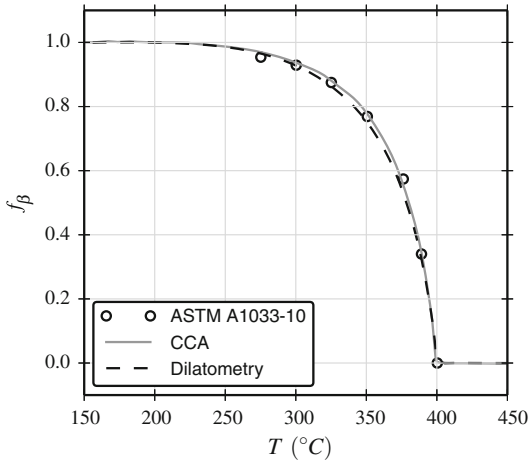

Fig. 5—A comparison of the two fraction transformed curves and the values from the ASTM standard.

VI. DISCUSSION

In the analysis presented here, mass fractions are used because mass is a conserved quantity. With information about phase densities, a conversion to volume fraction is straightforward.

Both techniques can be applied simultaneously to the sample. All forms of dilatometry and CCA rely on some form of baseline. In the case of martensitic transformations, the baseline at low temperatures can contain a small error because the martensitic transformation is often not 100 pct finished at the lowest measured temperature. Both methods are also susceptible to inaccuracies due to temperature gradients within the sample which is discussed in detail in the Appendix (although these will be small due to the relatively small size of the sample).

The primary difference between the two methods is that the response variable is measured *directly* in the dilatometry analysis; compared to CCA, in which the response variable (heat flux away from the sample) is *inferred* based on temperature measurements and known heat transfer analysis methods. This has the potential to

lead to inaccuracy if the heat transfer model does not accurately describe the experimental setup; however, the authors have found that it is relatively easy to create an experiment that can be well described by either a convective or radiative heat transfer law. This could make dilatometry more appealing if the transformation of interest occurs in a temperature range in which the dominant heat transfer mechanism changes; for example, from radiative at high temperatures to convective at lower temperatures.

The primary advantage of CCA is in the simplicity of its experimental setup and the freedom that this affords. One example of this flexibility is in the experiments presented here. These experiments were setup as standard dilatometry experiments without modifications for the CCA. With the analysis that was done here, relatively little new information was gained but by having two sources of information (length and heat) it would be possible to use the differences in these data to gain more information out of these experiments. For example, the length measurement is along one direction *vs* heat that is omni-directional so some estimate of anisotropy could be made; or heat evolved is a combination of heat released by the transformation and heat absorbed by new interfaces being generated, so an estimate of the amount of interfacial energy in the sample could be made.

VII. CONCLUSIONS

A sample of 9Cr3W3CoVNb steel was processed by normalizing at 1423 K (1150 °C) for 1 hour, subsequently tempering at 1043 K (770 °C) for 4 hours. This sample was exposed to a simulated weld thermal cycle by rapidly heating it to 1373 K (1100 °C) and finally free cooling in a Bahr DIL-805/D dilatometer, resulting in a microstructure of nearly 100 pct martensite.

CCA has proven to be quite effective at producing similar results to dilatometry despite its drastically simpler experimental setup. CCA has also almost exactly reproduced the evolution of the martensitic transformation, as determined by dilatometry. The result of this experiment supports CCA as a complement to dilatometry with the ability of tracking phase transformations even in the absence of dimensional changes. This, combined with the interesting possibilities that can come from combining CCA with other experimental techniques, makes CCA an analysis tool with vast potential for future utilization and development.

ACKNOWLEDGMENTS

The authors would like to acknowledge the Natural Sciences and Engineering Research Council of Canada (NSERC), Codes And Standards Training Institute (CASTI) and MITACS for their support of this exploratory work.

APPENDIX: ESTIMATION OF TEMPERATURE GRADIENTS IN A DILATOMETRY SAMPLE

Typically in dilatometry, the temperature is measured with a thermocouple welded to the surface of the metal sample. During free cooling of a metal dilatometry sample, a slight difference exists between the temperature of the core of the sample and its surface.

From an energy balance on the surface of the sample (heat transfer due to conduction equal to heat transfer due to convection) and assuming heat losses are only through the sides of the cylindrical sample, which is typically the case in a push rod dilatometer, Eq. [16] can be rewritten as:

$$\frac{\mathrm{d}T}{\mathrm{d}t}\left[mc_{\mathrm{p}}^{\alpha}(1-f_{\beta})+mc_{\mathrm{p}}^{\beta}f_{\beta}-m\Delta H^{*}\frac{\partial f_{\beta}}{\partial T}\right] = \bar{h}A(T-T_{\infty})=-kA\left.\frac{\partial T}{\partial r}\right|_{R}. \quad [A1]$$

This equation can then be simplified to:

$$m\bar{c_{\mathrm{p}}}\frac{dT}{dt}=-kA\left.\frac{\partial T}{\partial r}\right|_{R}. \quad [A2]$$

In this case $\bar{c_{\mathrm{p}}}$ is the average heat content in the transformation range $\left(\bar{c_{\mathrm{p}}}=\frac{H_2^*-H_1^*}{T_2-T_1}\right)$, where H_2^* and T_2 relate to the enthalpy and temperature at the start of the transformation and H_1^* and T_1 relate to values at the end of the transformation. The corresponding thermal diffusivity is $\bar{\alpha}=\frac{k}{\rho\bar{c_{\mathrm{p}}}}$. Values for the thermophysical properties used in this calculation are listed in Table IV. Temperature homogeneity is crucial to the analysis techniques presented here. The degree to which a sample is spatially isothermal is captured by the Biot number ($\mathrm{Bi}=\frac{\bar{h}R}{k}$).[19] For small Bi numbers $\left(\frac{\bar{h}R}{k}\ll 1\right)$, the temperature profile can be considered to be nearly homogeneous, decreasing uniformly at all points with time.[20] A nearly uniform temperature distribution can be captured well with a second order polynomial. According to Reference 21, the gradient at the surface could then be estimated as:

$$-\left.\frac{\partial T}{\partial r}\right|_{R}\approx 2\frac{\Delta T_{\max}}{R} \quad [A3]$$

Considering a long cylinder:

$$m=\pi R^2 L\rho,\quad A=2\pi RL, \quad [A4]$$

then,

Table IV. List of Values Used in Temperature Gradient Calculation

Quantity	Value	Units	Reference
k	22.3	W/mK	[22, 23]
ρ	7645	kg/m^3	[22]
$\bar{c_{\mathrm{p}}}$	601	J/kg K	[24, 25]
$\bar{\alpha}$	4.85×10^{-6}	m^2/s	
$\bar{h}$	19.1	W/m^2 s	
R	0.002	m	

$$\Delta T_{\max} \approx \frac{1}{4}\frac{R^2}{\bar{\alpha}}\frac{\mathrm{d}T}{\mathrm{d}t} \qquad [A5]$$

The value of $\bar{h}$ was estimated from the high temperature, single phase data using a value of $c_p \approx 500\,\mathrm{J/kg\,K}$.[24,25] A value for $\bar{c_p}$ was determined by using a transformation temperature range of 225 °C to 400 °C. Using Eq. [A5], the maximum temperature difference is $\Delta T_{\max} \approx 0.1\,^{\circ}\mathrm{C}$ in the transformation temperature regime, indicating that the spatially isothermal assumption is valid.

REFERENCES

1. T.C. Tszeng and G. Shi: *Mater. Sci. Eng. A*, 2004, vol. 380, pp. 123–36.
2. A.I.Z. Farahat: *J. Mater. Process. Technol.*, 2008, vol. 204, pp. 365–69.
3. A. Bojack, L. Zhao, P. Morris, and J. Sietsma: *Mater. Charact.*, 2012, vol. 71, pp. 77–86.
4. A. Kiani-Rashid and D. Edmonds: *Mater. Sci. Eng. A*, 2008, vols. 481–482, pp. 752–56.
5. J.W. Gibbs and P.F. Mendez: *Scripta Mater.*, 2008, vol. 58, pp. 699–702.
6. J.W. Gibbs, M.J. Kaufman, R.E. Hackenberg, and P.F. Mendez: *Metall. Mater. Trans. A*, 2010, vol. 41A, pp. 2216–23.
7. R.C. MacKenzie: *Differential Thermal Analysis*, Academic Press, London, 1970.
8. B.T. Alexandrov and J.C. Lippold: *Weld. World*, 2007, vol. 51, pp. 48–59.
9. J. Tamminen: Ph.D. Thesis, University of Stockholm, 1988.
10. M. Kiuchi and S. Sugiyama: *Ann. CIRP*, 1994, vol. 43, pp. 271–74.
11. S.I. Bakhtiyarov, M. Dupac, R.A. Overfelt, and S.G. Teodorescu: *J. Fluids Eng.*, 2004, vol. 126, pp. 468–70.
12. J.I. Frankel, W.D. Porter, and A. Sabau: *J. Therm. Anal. Calorim.*, 2005, vol. 82, pp. 171–77.
13. D.M. Stefanescu, G. Upadhya, and D. Bandyopadhyay: *Metall. Trans. A*, 1990, vol. 21A, pp. 997–1005.
14. P. Mayr: Ph.D. Thesis, Graz University of Technology, 2007.
15. P. Mayr, T. Palmer, J. Elmer, E. Specht, and S. Allen: *Metall. Mater. Trans. A*, 2010, vol. 41A, pp. 2462–65.
16. P. Mayr: *Weld. World*, 2013, vol. 54, pp. R1–R11.
17. P. Mayr, T.A. Palmer, J.W. Elmer, and E.D. Specht: *Int. J. Mater. Res.*, 2008, vol. 99, pp. 381–86.
18. ASTM A1033-10: *Referencing: ASTM International, Designation: A* 1033–10, pp. 1–14, 2013.
19. T.L. Bergman, F.P. Incropera, A.S. Lavine, and D.P. DeWitt: *Fundamentals of Heat and Mass Transfer*, Wiley, New York, 2011.
20. D.R. Poirier and G.H. Geiger: *Transport Phenomena in Materials Processing*, Wiley, New York, 2013.
21. P.F. Mendez: *J. Appl. Mech.*, 2010, vol. 77, p. 61017112.
22. JAHM: Material Property Database (MPDB v6.61), 1999.
23. M. Peet, H. Hasan, and H. Bhadeshia: *Int. J. Heat Mass Transf.*, 2011, vol. 54, pp. 2602–08.
24. Thermo-Calc Software TCFE6 Steels/Fe-alloys database Version 6.2, 2013.
25. M. Gojić, M. Sućeska, and M. Rajić: *J. Therm. Anal. Calorim.*, 2004, vol. 75, pp. 947–56.